Talanta 115 (2013) 143–149

Contents lists available at ScienceDirect

Talanta

journal homepage: www.elsevier.com/locate/talanta

Using the iPhone as a device for a rapid quantitative analysis of trinitrotoluene in soil

Aree Choodum [a,b,*], Proespichaya Kanatharana [b,c], Worawit Wongniramaikul [b,d,e], Niamh Nic Daeid [f]

[a] *Department of Applied Science, Faculty of Science, Prince of Songkla University, Hat Yai, Songkhla 90112 Thailand*
[b] *Trace Analysis and Biosensor Research Center, Prince of Songkla University, Hat Yai, Songkhla 90112 Thailand*
[c] *Department of Chemistry and Center of Excellence for Innovation in Chemistry, Faculty of Science, Prince of Songkla University, Hat Yai, Songkhla 90112 Thailand*
[d] *Faculty of Technology and Environment, Prince of Songkla University, Phuket Campus, Phuket 83120 Thailand*
[e] *Center of Excellence for Environmental and Hazardous Waste Management (EHWM), Southern University Consortium, Prince of Songkla University, Hat Yai, Songkhla 90112 Thailand*
[f] *Centre for Forensic Science, Department of Pure and Applied Chemistry, WestCHEM, University of Strathclyde, 204 George Street, Glasgow G1 1WX, UK*

ARTICLE INFO

Article history:
Received 25 December 2012
Received in revised form
12 April 2013
Accepted 16 April 2013
Available online 29 April 2013

Keywords:
Digital images
Red Green Blue color system
iPhone
Trinitrotoluene

ABSTRACT

Mobile ‘smart’ phones have become almost ubiquitous in society and are typically equipped with a high-resolution digital camera which can be used to produce an image very conveniently. In this study, the built-in digital camera of a smart phone (iPhone) was used to capture the results from a rapid quantitative colorimetric test for trinitrotoluene (TNT) in soil. The results were compared to those from a digital single-lens reflex (DSLR) camera. The colored product from the selective test for TNT was quantified using an innovative application of photography where the relationships between the Red Green Blue (RGB) values and the concentrations of colorimetric product were exploited. The iPhone showed itself to be capable of being used more conveniently than the DSLR while providing similar analytical results with increased sensitivity. The wide linear range and low detection limits achieved were comparable with those from spectrophotometric quantification methods. Low relative errors in the range of 0.4 to 6.3% were achieved in the analysis of control samples and 0.4–6.2% for spiked soil extracts with good precision (2.09–7.43% RSD) for the analysis over 4 days. The results demonstrate that the iPhone provides the potential to be used as an ideal novel platform for the development of a rapid on site semi quantitative field test for the analysis of explosives.

1. Introduction

The development of affordable multifunctional mobile phone devices has occurred very rapidly over recent years. Such devices have become more technically sophisticated and are being routinely used for purposes outside of basic communication, for example in healthcare-related applications [1–5]. A typical mobile phone is also equipped with a high-resolution digital camera and various camera options are available, such as autofocus, digital zoom and white balance. This has made it more convenient for the user to take photographs using ‘built-in’ digital cameras in a mobile phone instead of other high quality portable digital cameras.

The use of digital imaging and particularly digital cameras for quantitative colorimetric testing has been recommended in various applications [6–14]. These uses are based on the measurement of the shades of colorimetric products in digital images made for the test. Although color is subjective, the use of color spaces and imaging devices facilitates the use of color for quantification [15].

Recently, rapid quantitative analysis of trinitrotoluene (TNT) using Nessler's test coupled with digital image analysis has been reported [14]. A powerful method with the capability to be deployed as a rapid field test has been successfully performed using a digital single-lens reflex (DSLR) camera for capturing an image of the color products from the test.

In this work, a built-in digital camera in a mobile phone was introduced instead of DSLR camera. The use of the digital camera within the ‘smart’ phone was selected to facilitate the development of a portable rapid quantitative chemical analysis system as a readily available portable field device. The use of a smart phone could include the development of Java support and options for

---

* Corresponding author at: Department of Applied Science, Faculty of Science, Prince of Songkla University, Hat Yai, Songkhla 90112 Thailand.
Tel.: +66 7428 8102; fax: +66 7444 6681.
E-mail address: aree.c@psu.ac.th (A. Choodum).

0039-9140/$ - see front matter © 2013 Elsevier B.V. All rights reserved.
http://dx.doi.org/10.1016/j.talanta.2013.04.037

installing and running externally developed applications (apps) which would provide the end user readout in relation to sample analysis. The performance of the built-in digital camera within an iPhone was compared to that of DSLR camera in order to establish the feasibility of using an iPhone as a field analytical detector. The study analyzed control and field samples for the presence of TNT which is one of the most widely deployed explosive materials in a global sense. Rapid cost effective field tests for TNT are often required because of the prevalence of this material in land and ground water contaminated because of their proximity to military dumping sites [16] as well as the use of such materials in improvised explosive devices and conventional milatary ordinance.

2. Materials and methods

2.1. Color test of TNT

2, 4, 6-Trinitrotoluene in acetonitrile (1 mg mL^{-1}) (Supelco, PA) was purchased and used as the stock solution. The stock solution was further diluted with acetone to appropriate concentrations in the range of 1 to 1000 mg L^{-1} to produce a range of TNT standards. A TNT color test was performed using dicyclohexylamine (DCHA; Aldrich, WI) as the electron donating reagent [16]. Twenty microliters of each TNT standard solution was transferred to a micro-centrifuge tube and 50% dicyclohexylamine in acetone was added as the test reagent to obtain a red–violet product. The volume of test reagent was optimized to determine the volume required to produce the darkest color reaction for the least concentrated analyte solution. The resultant colors were photographed one minute after color development using the built-in digital camera of an iPhone 4.0 and an Olympus E330 digital camera (17.3 × 13.0 mm^2 with a 12-bit RGB Live MOS sensor).

Each color test was repeated 3 times across all concentrations of prepared standards and each resultant color was photographed six times by each digital camera. The average intensities of the red, green and blue colors from each of the 6 images obtained for each standard solution were investigated using Adobe Photoshop and a calibration graph prepared for each color. The limit of detection was calculated using standard methods [17] and precision was expressed as a percentage of the relative standard deviation of the RGB values for each color from the 6 analyzed images.

2.2. Photographic system

A simple photographic system was set up in a 25 × 22 × 22-in. opaque safety cabinet which had a white interior in order to obtain the same environmental light conditions for both devices. Colored products generated from the TNT test were photographed as described by each device and under the same lighting conditions. The Olympus digital camera was set at optimized exposure conditions to obtain the best determination performances, *i.e.* automatic focus, automatic white balance, automatic sensitivity (where the ISO speed was set within 100–400), and used in single image mode. Each image was 1.34 MB (3136 × 2352-pixel) and was saved as a JPEG (24-bits). The built-in digital camera of the iPhone 4.0 was set to flash ‘off’ with the high dynamic range (HDR) on, and recorded for both the original and enhanced images. Each image was 2.0 MB (2592 × 1936-pixel) and was saved as a JPEG (24-bits) on the iPhone's memory.

Once the images were transferred to a computer, they were opened in Adobe Photoshop CS3. The photograph depicting each color product in each micro-centrifuge tube was cropped to the middle of the image to approximately 35 × 30-pixels. The red, green, and blue color intensities of the cropped area were then obtained by using the ‘histogram’ tool. The data were transferred to an Excel (version 2007) spreadsheet for subsequent data analysis. The RGB intensities from three micro-centrifuge tubes of 6 repetitive images were averaged and used as one point in all graphs.

2.3. Color test of TNT in soil sample

The color test of the TNT in the soil sample was performed following the procedure used in our previous study [14]. A soil sample (1 g) was extracted using 2.5 mL of acetone after sonication for 15 min followed by filtration using Whatman No.1 filter paper. The resulting filtrate was spiked with a TNT standard solution in order to investigate the effect of the color of the soil filtrate on the TNT test color derived from the test. The extracted solution was analyzed using the DCHA test and all extractions and analyzes were repeated in triplicate and over a four day period. Concentrations of TNT in the extracted samples were quantified using the linear calibration graph of both developed methods. The relative errors between spiked concentration and quantified concentration were examined.

3. Results and discussion

3.1. TNT color test

Red–violet products were observed from the DCHA test for the presence of TNT. The formation of the colored product is based on a charge-transfer mechanism [16,18] in which the DCHA acts as an electron donor and TNT acts as an electron acceptor as suggested by Ercag et al. [18]. No color change was observed for the DCHA test in the presence of dinitrotoluene (2,4-DNT or 2,6-DNT) or dinitrobenzene (1,3-DNB) confirming that the test was selective for TNT. A color change was observed with tetryl but produced an orange color easily distinguished from the red–violet product of the TNT complex [18].

The darkness of the red–violet product generated by the reaction could be related to the concentration of TNT present facilitating the development of an objective semi quantitative analytical methodology.

3.2. The analysis of digital images for the quantification of TNT

A color space is required to specify the color of the test product [15,19] and both digital cameras used the sRGB color space which is a device-independent. Both digital cameras use internal calibration data to transform the measured RGB values into the sRGB color space so that the same color is produced on every device [20,21]. Thus, both devices were expected to provide the same color for the test products photographed. Images transferred to Adobe Photoshop also retain their RGB since Photoshop automatically recognizes the color space of the picture [22]. The R(ed), G(reen), and B(lue) intensities obtained from analyzing the digital image representing the total photons in each region of the spectrum [15] were used for quantification.

It should be noted that the colors obtained from each of the three channels (RGB) are subtractive colors and selectively absorb certain wavelengths of light (*i.e.* 400–500, 500–580, and 580–700 nm for the blue, green, and red channel, respectively [15]), and thus affect the observed color [7,13,23]. The eye sees the converse of the color component that is primarily absorbed [7]. As a consequence, the red–violet color produced in the TNT test was expected to reflect or transmit red and blue light and absorb green light.

Red–violet products of TNT were photographed with the DSLR at optimized exposure conditions [12–14]. Because most of

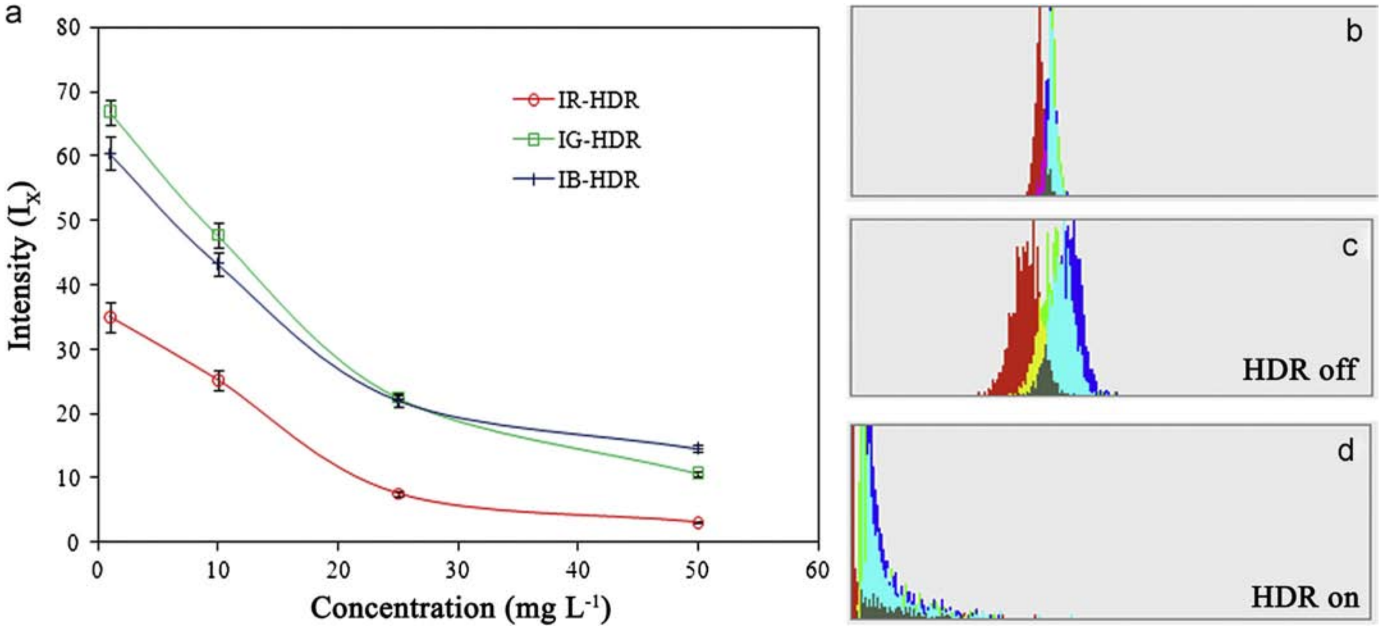

Fig. 1. (a) Relationship between individual RGB values and TNT concentration of iPhone digital images with high dynamic range (b) histogram of 50 mg L^{-1} TNT color product from DSLR's image (c) original iPhone image (d) and HRD iPhone image.

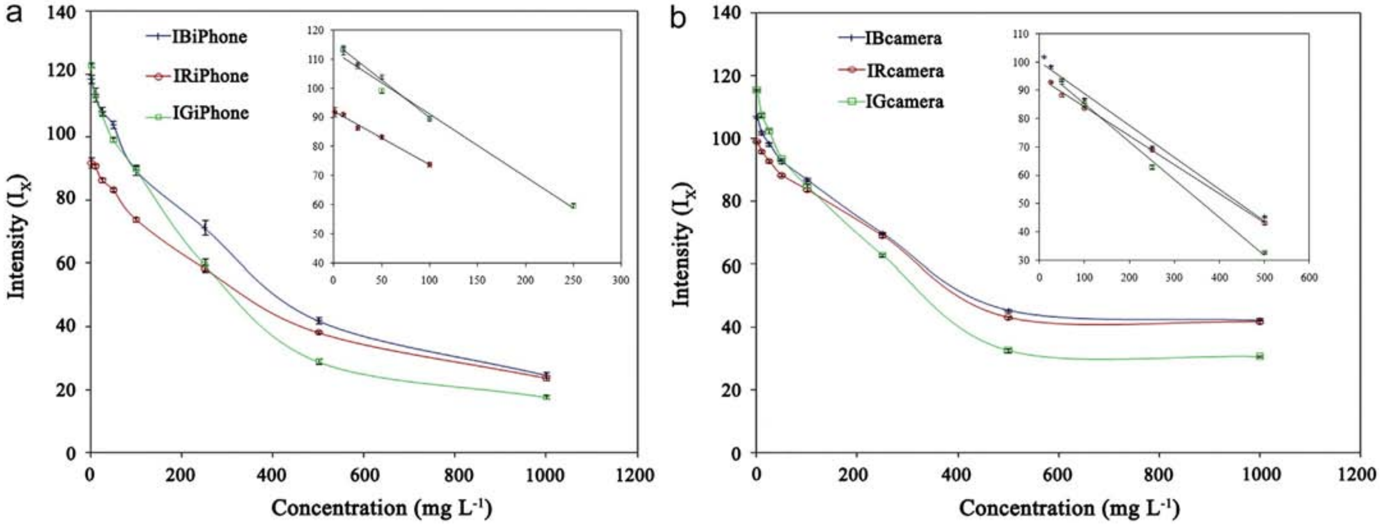

Fig. 2. Relationship between individual RGB intensity values and TNT concentration (a) DSLR (b) iPhone images.

exposure parameters did not affect the determination performance [11], they were set at automatic focus, automatic white balance, and automatic sensitivity for convenience.

For the built-in digital camera of the iPhone, the products were imaged with the HDR on, and recorded both as original and enhanced images. HDR images looked grainy when compared to the original images. This was probably because the HDR image of the iPhone combines three images capturing at different exposures, (underexposed, normal, and overexposed). However the photographic system that was used did not include a specific light source that may have affected the exposure conditions. The TNT color product in the HDR images appeared to be underexposed as all three colors moved toward the left side of the histogram (Fig. 1d) compared to the original images (Fig. 1c), and the DSLR images (Fig. 1b). Color intensities of the enhanced images of the products of TNT at various concentrations (Fig. 1a) also had a narrower linear determination range (1–25 mg L^{-1}). As a consequence of these observations the original rather than HRD iPhone images were used to compare with the DSLR images.

The overall trends in the relationship between the intensities of the red and blue light and the TNT concentration from both cameras was similar as both were reflected by the colored products, where as more pronounced differences were observed for the absorbed green light (Fig. 2a-b). Over a TNT concentration range of 1 to 500 mg L^{-1} of TNT, the intensities of green (I_G) (Fig. 3b) and blue light (I_B) (Fig.3c) from both the digital cameras were similar, while the intensity of red light (I_R) from the iPhone camera (original images) was always lower than that obtained from the DSLR camera (Fig.3a). Although the backside illumination (BSI) CMOS image sensor was used in the iPhone 4.0 [24–25], which allows more incident light to reach the light sensing silicon [26–27], its size is smaller than those present within the DSLR's. The intensities of all channels from the DSLR camera were constant across a TNT concentration range from 500 to

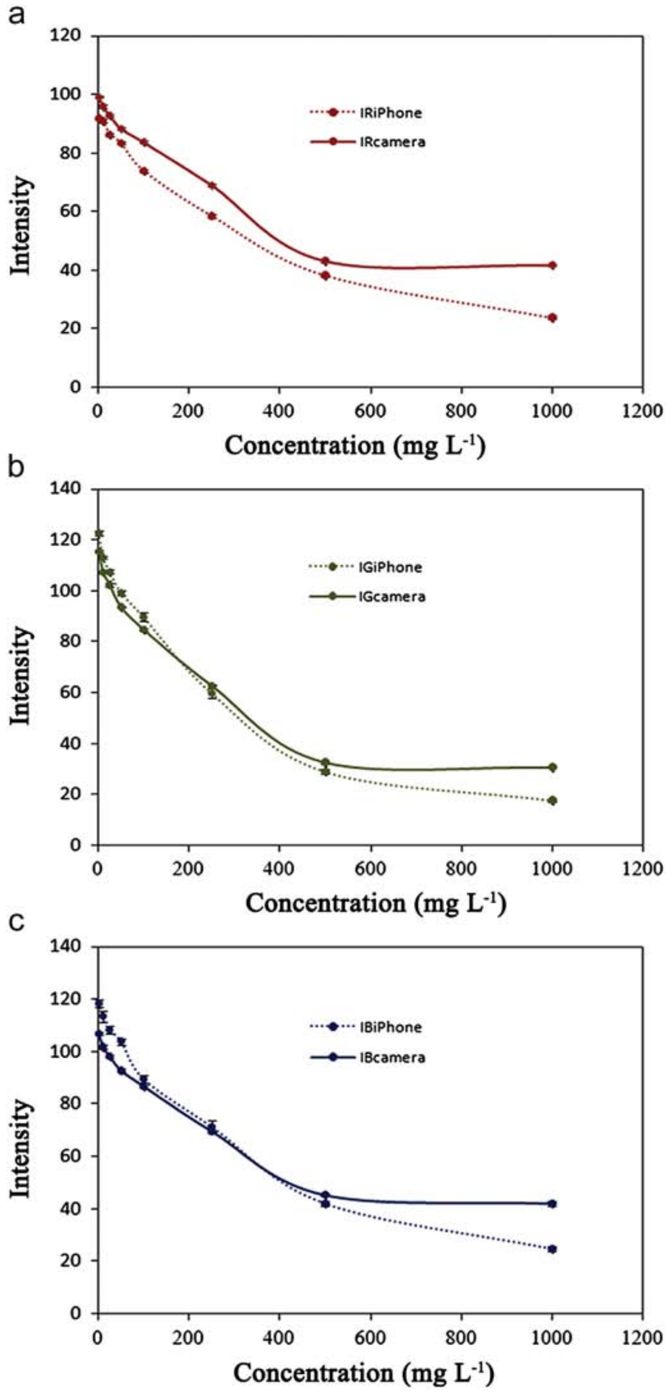

Fig. 3. Relationship between (a) intensity of red light (b) intensity of green light (c) intensity of blue light and TNT concentration from DSLR and iPhone images.

1000 mg L^{-1} revealing a clear difference from the iPhone's built-in camera which had lower intensities. The larger sensor of DSLR seems to increase the opportunity of photons to be registered even when less photons were reflected from a darker product and resulted in an overall increase in intensity with the DSLR images. However, the BSI CMOS sensor of the iPhone demonstrated a better ability to detect small differences in photon emission from darker products, while no difference was observed from the DSLR for the same samples. This was most likely because the light could strike the photocathode layer without passing through the wiring layer in the BSI CMOS sensor providing better sensitivity [26–27].

The molecular absorption of the colored products was calculated using an equation described in previous studies [12,13,28] and green light was found to have the highest level of absorbance. The spectral responsivity of the green channel was typically in the range of 500 to 580 nm [15]. This result was in agreement with previous studies that reported λ_{max} of this complex at 531 nm [16] and 530 nm [18]. The absorbance of the TNT complex from the DSLR camera images increased with TNT concentration from 1 to 500 mg L^{-1} as expected before becoming constant (Fig.4a). This finding was similar to previous results [12–14] and corroborates results typically obtained from a spectrophotometer. The calculated absorbance from the iPhone images continued to increase from 500 to 1000 mg L^{-1} TNT, although not in a linear fashion (Fig.4b), which was probably due to the improved sensitivity of the image sensor as previously described. The absorption profiles of the blank corrected TNT complex for the iPhone images and the DSLR camera images are shown in respectively Fig. 4d and Fig. 4c.

The total RGB values *i.e.* the total intensity ($I_{TOTAL}=I_R+I_G+I_B$) and the total absorbance ($A_{TOTAL}=A_R+A_G+A_B$) of both cameras (Fig. 5) were also compared because these would provide more valuable information in addition to the individual RGB values [8,13]. Both the total values of the iPhone and DSLR camera images were very similar at low concentrations of TNT (1–50 mg L^{-1}), differentiating at higher concentrations (100 mg L^{-1} and specifically at 1000 mg L^{-1}). These differences were also observed for blank corrected images.

3.3. Analytical performance and validation

The linear range, calibration equation, and linearity of the developed method are summarized in Table 1, while other analytical performances, *i.e.* sensitivity, precision, and accuracy are shown in Table 2. The linear correlations between RGB absorbance and TNT concentration were observed in the range of 1 to 500 mg L^{-1} of TNT using both the DSLR and iPhone cameras. Shorter concentration ranges were used for RGB intensity. These concentration ranges were wider than previously reported using a spectrophotometer (5–50 mg L^{-1}) [18] and our previous digital image analysis (1–50 mg L^{-1}) [14]. The greater analytical range was thought to be due to the use of DCHA as the colorimetric reagent rather than Nessler's reagent which had been previously reported [14]. Better sensitivity (higher slope of the calibration equation) was revealed with the iPhone imaging rather than the DSLR camera. This was because of the use of the BSI CMOS image sensor as previously mentioned and indicated that the BSI image sensor of the iPhone provided an overall better ability to detect small changes within the color product of TNT, even though the sensor size was smaller. The repeatability of inter-day analysis ($n=4$) were in the range of 2.09 to 7.43% RSD and 0.11 to 5.75% RSD for the iPhone and the DSLR camera, respectively (Table 2). Accuracy was evaluated based on the percentage relative error ($(x_e - x_c)/x_c \times 100$) in the analysis of a control sample of known concentration of TNT standard solution ($x_c = 75$ mg L^{-1}) quantified using an external calibration (x_e) and was found to be less than 6.3%. The detection limit, taken as the TNT concentration giving a signal equal to the blank signal plus three standard deviations of the blank [17], for the determination of TNT using the DSLR camera imaging were in the range of 0.464 ± 0.001 mg L^{-1} to 6.8 ± 0.1 mg L^{-1} which was in line with those recently reported using colorimetry coupled with spectrophotometric detection (3 mg L^{-1}) [18]. By the iPhone built-in digital camera imaging, the detection limit of the determination method was 3.76 ± 0.08 to 4.0 ± 0.1 mg L^{-1} for green light, which were close to 3 mg L^{-1} of previously reported data [18].

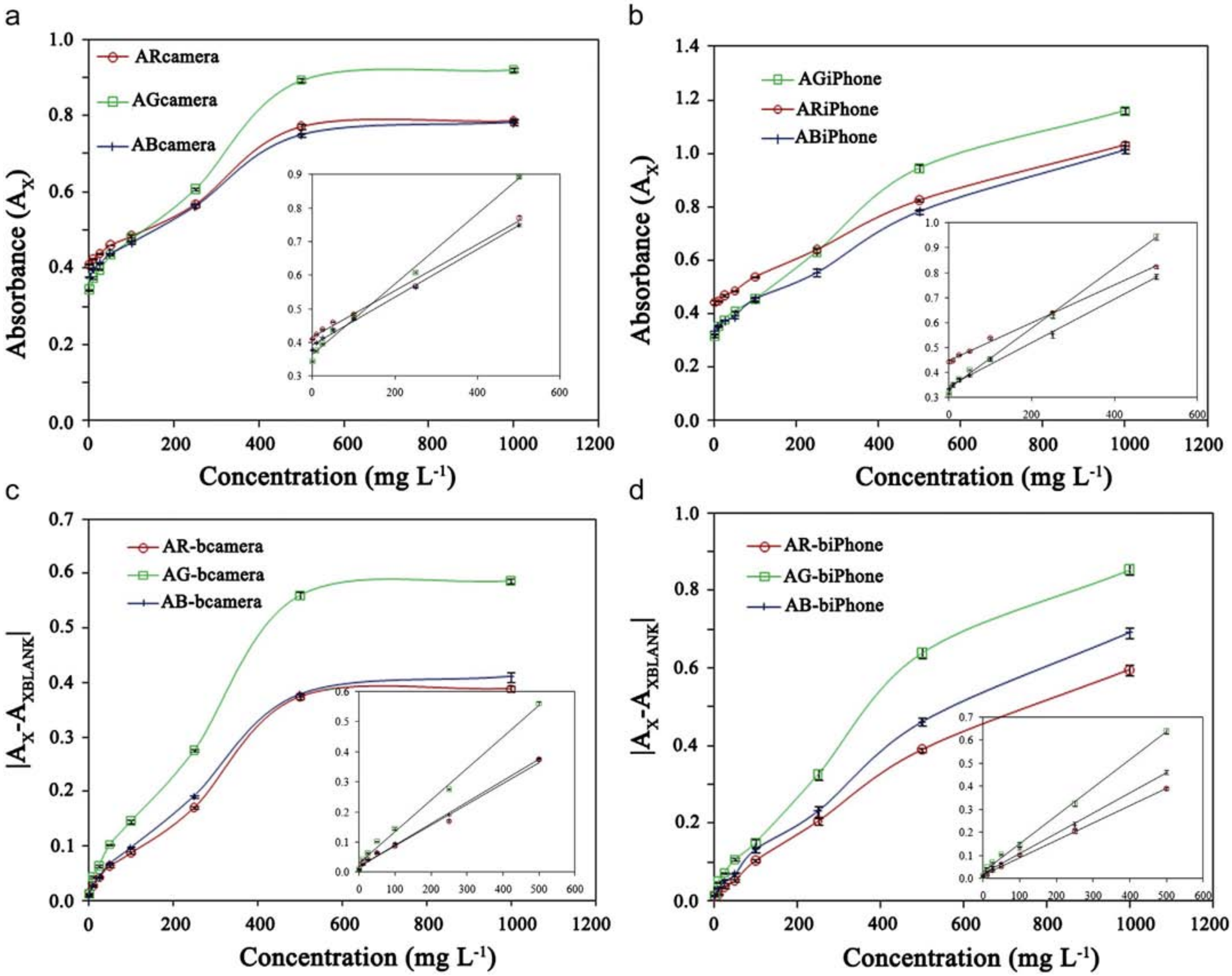

Fig. 4. Relationship between absorbance of RGB values and TNT concentration (a) DSLR image without blank subtracted (b) iPhone image without blank subtracted (c) DSLR image with blank subtracted (d) iPhone image with blank subtracted.

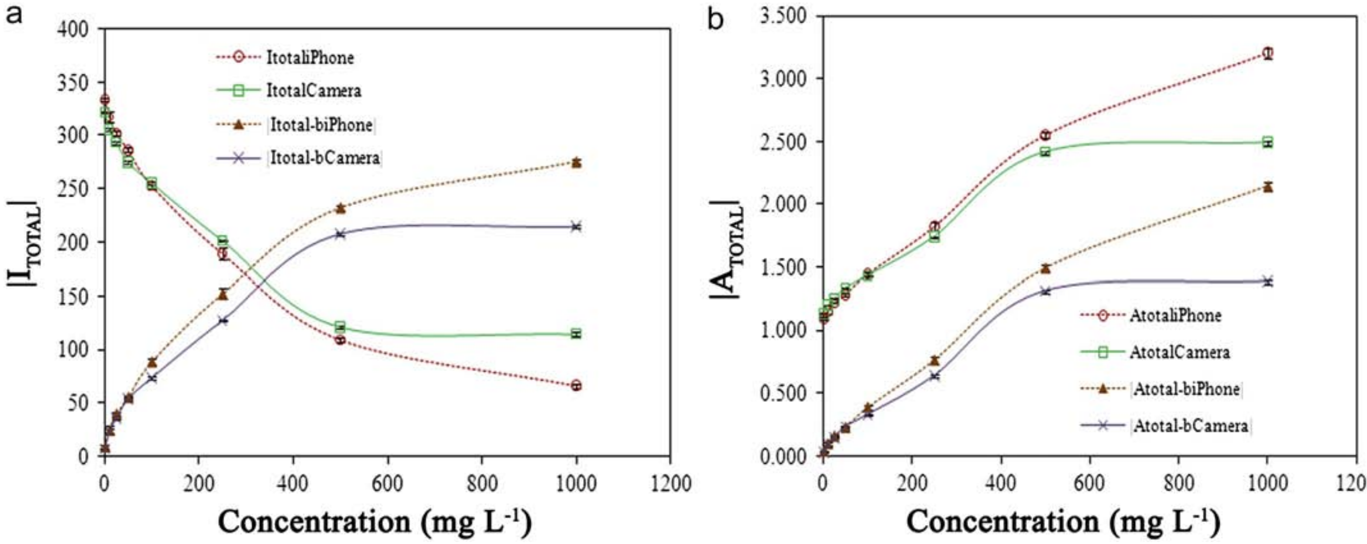

Fig. 5. Relationship between total RGB values (with and without blank subtracted) and TNT concentration (a) total intensity (b) total absorbance.

Table 1
Linear ranges and calibration equations of methods using DSLR and iPhone for capture product images.

Parameter	Linear range (mg L^{-1})		Calibration equation (y=unit, x=mg L^{-1})		Linearity (R^2)	
	iPhone	DSLR	iPhone	DSLR	iPhone	DSLR
I_R	1–100	25–500	$y=(0.19\pm0.01)x+(92.0\pm0.5)$	$y=(0.102\pm0.002)x+(94.3\pm0.6)$	0.9907	0.9986
I_G	10–250	50–500	$y=(0.22\pm0.01)x+(112\pm2)$	$y=(0.134\pm0.006)x+(99\pm2)$	0.9901	0.9958
I_B	10–100	10–500	$y=(0.26\pm0.02)x+(115.8\pm0.9)$	$y=(0.1121\pm0.006)x+(100\pm1)$	0.9922	0.9897
A_R	1–500	1–500	$y=(0.00080\pm0.00003)x+(0.449\pm0.006)$	$y=(0.00070\pm0.00003)x+(0.416\pm0.006)$	0.9973	0.9925
A_G	1–500	1–500	$y=(0.00120\pm0.00003)x+(0.336\pm0.006)$	$y=(0.00100\pm0.00004)x+(0.36\pm0.01)$	0.9974	0.9943
A_B	1–500	1–500	$y=(0.00090\pm0.00003)x+(0.346\pm0.007)$	$y=(0.00070\pm0.00002)x+(0.392\pm0.005)$	0.9948	0.9956
$\|I_R-I_{R\mathrm{blank}}\|$	1–100	1–500	$y=(0.178\pm0.008)x+(2.01\pm0.4)$	$y=(0.107\pm0.004)x+(6\pm1)$	0.9933	0.9913
$\|I_G-I_{G\mathrm{blank}}\|$	10–250	50–500	$y=(0.22\pm0.01)x+(14\pm2)$	$y=(0.134\pm0.006)x+(20\pm2)$	0.9901	0.9958
$\|I_B-I_{B\mathrm{blank}}\|$	10–100	10–500	$y=(0.26\pm0.02)x+(5.8\pm0.9)$	$y=(0.112\pm0.006)x+(8\pm1)$	0.9922	0.9897
$\|A_R-A_{R\mathrm{blank}}\|$	1–500	1–500	$y=(0.00080\pm0.00003)x+(0.015\pm0.006)$	$y=(0.00070\pm0.00003)x+(0.018\pm0.006)$	0.9977	0.9925
$\|A_G-A_{G\mathrm{blank}}\|$	1–500	1–500	$y=(0.001200\pm0.000006)x+(0.031\pm0.002)$	$y=(0.00100\pm0.00004)x+(0.03\pm0.01)$	0.9974	0.9943
$\|A_B-A_{B\mathrm{blank}}\|$	1–500	1–500	$y=(0.00090\pm0.00003)x+(0.023\pm0.007)$	$y=(0.00070\pm0.00002)x+(0.020\pm0.005)$	0.9948	0.9956
I_{TOTAL} ($I_R+I_G+I_B$)	10–100	25–500	$y=(0.70\pm0.04)x+(322\pm2)$	$y=(0.36\pm0.02)x+(294\pm4)$	0.9938	0.9941
A_{TOTAL} ($A_R+A_G+A_B$)	1–500	1–500	$y=(0.00280\pm0.00006)x+(1.13\pm0.01)$	$y=(0.00250\pm0.00008)x+(1.17\pm0.02)$	0.9979	0.9948
$\|(I-I_{\mathrm{blank}})\|_{\mathrm{TOTAL}}$	10–100	25–500	$y=(0.70\pm0.04)x+(20\pm2)$	$y=(0.36\pm0.02)x+(34\pm4)$	0.9948	0.9941
$\|(A-A_{\mathrm{blank}})\|_{\mathrm{TOTAL}}$	1–500	1–500	$y=(0.00280\pm0.00006)x+(0.07\pm0.01)$	$y=(0.00250\pm0.00008)x+(0.07\pm0.02)$	0.9980	0.9948

Table 2
Analytical performance of methods using DSLR and iPhone for capture product images.

Parameter	Sensitivity (unit/(mg L^{-1}))		Precision (%RSD of 4 days analysis)		% Relative error[a] (75 mg L^{-1} control)		% Relative error (50 mg L^{-1} spiked soil)	
	iPhone	DSLR	iPhone	DSLR	iPhone	DSLR	iPhone	DSLR
I_R	0.19 ± 0.01	0.102 ± 0.002	2.24	2.42	+5.7	+0.6	−3.0	−0.4
I_G	0.22 ± 0.01	0.134 ± 0.006	3.65	3.14	+2.6	−0.6	+1.7	+0.02
I_B	0.26 ± 0.02	0.1121 ± 0.006	6.74	5.32	+4.8	−1.9	+5.6	+1.4
A_R	0.00080 ± 0.00003	0.00070 ± 0.00003	2.21	2.63	+5.8	−2.2	−5.6	−1.1
A_G	0.00120 ± 0.00003	0.00100 ± 0.00004	4.34	3.51	−1.7	−0.7	+6.2	+0.9
A_B	0.00090 ± 0.00003	0.00070 ± 0.00002	7.43	5.75	+6.3	0.0	+4.0	+2.7
$\|I_R-I_{R\mathrm{blank}}\|$	0.178 ± 0.008	0.107 ± 0.004	6.06	3.21	+5.7	+0.6	+2.0	−0.4
$\|I_G-I_{G\mathrm{blank}}\|$	0.22 ± 0.01	0.134 ± 0.006	2.72	4.88	+2.7	+5.6	+1.5	+0.02
$\|I_B-I_{B\mathrm{blank}}\|$	0.26 ± 0.02	0.112 ± 0.006	7.27	3.61	+5.5	−1.9	+0.4	+1.3
$\|A_R-A_{R\mathrm{blank}}\|$	0.00080 ± 0.00003	0.00070 ± 0.00003	7.36	2.85	−0.7	−2.2	+1.4	−1.1
$\|A_G-A_{G\mathrm{blank}}\|$	0.001200 ± 0.000006	0.00100 ± 0.00004	5.23	1.67	−1.7	−0.7	−2.2	+0.7
$\|A_B-A_{B\mathrm{blank}}\|$	0.00090 ± 0.00003	0.00070 ± 0.00002	2.09	0.27	+6.3	0.0	−3.2	+2.7
I_{TOTAL} ($I_R+I_G+I_B$)	0.70 ± 0.04	0.36 ± 0.02	4.44	3.47	+1.6	−4.5	+2.8	+0.3
A_{TOTAL} ($A_R+A_G+A_B$)	0.00280 ± 0.00006	0.00250 ± 0.00008	4.81	3.81	−0.4	+4.2	−3.4	+4.8
$\|(I-I_{\mathrm{blank}})\|_{\mathrm{TOTAL}}$	0.70 ± 0.04	0.36 ± 0.02	2.29	1.1	+1.6	−4.5	+5.2	−1.9
$\|(A-A_{\mathrm{blank}})\|_{\mathrm{TOTAL}}$	0.00280 ± 0.00006	0.00250 ± 0.00008	2.93	0.11	−0.4	−3.6	−0.8	+4.9

[a] % relative error=$(x_e-x_c)/x_c\times100$, x_c=a known-concentration of TNT standard solution (75 mg L^{-1}), x_e=concentration of TNT quantified using external calibration.

3.4. Quantification of TNT in soil

The correlations between the RGB values and TNT concentration in soil were also investigated. A standard TNT solution was spiked into a soil extract (x_c=50 mg L^{-1}) in order to study the influence of the soil matrices on the resultant sample. The samples were then analyzed by both methods and the concentration of TNT was quantified using each linear calibration (x_e). Both cameras produced impressive results as presented in Table 2. The relative errors between the spiked concentration and the quantified concentration using the linear calibration graph of the developed method were in the range 0.4 to 6.2% for the iPhone camera and 0.4 to 4.9% for the DSLR camera. This indicated excellent performance by both cameras for the quantification of TNT in soil. The results for blue light contrasted with our previous study [14] in which the red–purple of the TNT Nessler's test products were affected by the orange-brown soil color. This may be due to the color of the soil extract (pale yellow in this work and orange-brown in previous work [14]) or the color of the resultant colorimetric test mixture obtained from DCHA and Nessler's tests.

4. Conclusion

Digital image based analysis of red–violet TNT-DCHA products was used for the quantification of TNT using a DSLR camera and the built-in digital camera of an iPhone. Various correlations of the RGB value and the TNT concentration were successfully established using both cameras with a wide linear range and a low detection limit. The built-in digital camera of the iPhone showed a better potential for use in digital image based analysis of TNT than the DSLR camera with low relative error, very good precision, and better sensitivity. This indicated great potential for the development of an accurate, rapid, portable and economically viable semi-quantitative test for the analysis of TNT using a mobile ‘smart’ phone. This study also provided valuable information for the future development of an app enabling a smart phone to be used as a complete analytical detector.

Acknowledgments

This work was supported by TRF-CHE grant (no. MRG5480125) supported by the Thailand Research Fund, the Commission on Higher Education, Faculty of Science, and Prince of Songkla University. Partial support was also provided by the Trace Analysis and Biosensor Research Center (TAB-RC), the Center for Innovation in Chemistry (PERCH-CIC) and the Higher Education Research Promotion and National Research University Project of Thailand, the Commission of Higher Education.

References

[1] B.A. Cadle, K.C. Rasmus, J.A. Varela, L.S. Leverich, rsquo, C.E. Neill, R.K. Bachtell, D.C. Cooper, Subst. Abuse 4 (2010) 21–33.
[2] F. Kong, J. Tan, Pervasive Mob. Comput. 8 (2012) 147–163.
[3] K. Patrick, W. Griswold, F. Raab, S. Intille, Am. J. Prev. Med. 35 (2008) 177–181.
[4] A.W. Martinez, S.T. Phillips, E. Carrilho, S.W. Thomas, H. Sindi, G.M. Whitesides, Anal. Chem. 80 (2008) 3699–3707.
[5] K. Senior, Lancet Oncol. 12 (2011) 429–430.
[6] E.d.N. Gaiao, V.L. Martins, W.d.S. Lyra, L.F.d. Almeida, E.C.d. Silva, M.C.U. Araujo, Anal. Chim. Acta. 570 (2006) 283–290.
[7] L. Byrne, J. Barker, G. Pennarun-Thomas, D. Diamond, S. Edwards, Trends Analyt. Chem. 19 (2000) 517–522.
[8] A. Lopez-Molinero, D. Linan, D. Sipiera, R. Falcon, Microchem. J. 96 (2010) 380–385.
[9] W. Silva Lyra, V.B. dos Santos, A.G.G. Dionízio, V.L. Martins, L.F. Almeida, E. NobregaGaiao, P.H.G.D. Diniz, E.C. Silva, M.C.U. Araujo, Talanta 77 (2009) 1584–1589.
[10] N. Maleki, A. Safavi, F. Sedaghatpour, Talanta 64 (2004) 830–835.
[11] Y. Suzuki, M. Endo, J. Jin, K. Iwase, M. Iwatsuki, Anal. Sci. 22 (2006) 411–414.
[12] A. Choodum, N. Nic Daeid, Drug Test. Anal. 3 (2011) 277–282.
[13] A. Choodum, N. Nic Daeid, Talanta 86 (2011) 284–292.
[14] A. Choodum, P. Kanatharana, W. Wongniramaikul, N. Nic Daeid, Forensic Sci. Int. 222 (2012) 340–345.
[15] K. Cantrell, M.M. Erenas, I. de Orbe-Paya, L.F. Capitan-Vallvey, Anal. Chem. 82 (2010) 531–542.
[16] A. Üzer, E. Erçag, R. Apak, Anal. Chim. Acta 534 (2005) 307–317.
[17] J.N. Miller, J.C. Miller, Statistic and Chemometric for Analytical Chemistry, 5th ed., Pearson Education Limited, Essex, 2005.
[18] E. Erçag, A. Üzer, R. Apak, Talanta 78 (2009) 772–780.
[19] B. Maund, Color, in Stanford encyclopedia of philosophy, Metaphysics research lab, Center for the study of Language and Information: Stanford, CA, 2006.
[20] J.Y. Hardeberg, Aquistion and reproduction of color images: Colorimetric and multispectral approaches, FL: Universal-Publishers Inc., Boca Raton, 2001.
[21] A. Ford, A. Roberts, Color space conversion, Available from: 〈http://www.poynton.com/ PDFs/coloureq.pdf〉, 1998 (accessed 12.12.2012).
[22] T. Dosdale, Colour management, Available from: 〈http://myweb.tiscali.co.uk/dosdale/dosdale/colour%20management.pdf〉, 2008 (accessed12.12.2012).
[23] E.J. Giorgianni, T.E. Madden, Digital ColorManagement: Encoding Solutions, AddisonWesley, USA, 1998.
[24] P. Tufegdzic, iPhone 4 drives adoption of BSI image sensors in smart phone, Available from: 〈www.isuppli.com/Home-and-Consumer-Electronics/News/Pages/iPhone-4-Drive-Adoption-of-BSI-Image-Sensors-in-Smart-Phones.aspx〉, 2010 (accessed 21.03.2012).
[25] P. Tufegdzic, iPhone 4 finally brings the BSI image sensor to the handset market, Available from: 〈www.isuppli.com/Home-and-Consumer-Electronics/News/Pages/iPhone-4- Finally-Brings-the-BSI-Image-Sensor-to-the-Handset-Market.aspx?PRX〉, 2010 (accessed 21.03.2013).
[26] P.K. Swain, D. Cheskis, Back-illuminated image sensors come to the forefront, Photonics Spectra, Available from: 〈http://www.photonics.com/Article.aspx?AID=34685〉, August (2008). (accessed 21.03.2012).
[27] R. Marinelli, E. Palange, Prog. Electromagnetics Res. B 31 (2011) 1–14.
[28] M. Kompany-Zareh, M. Mansourian, F. Ravaee, Anal. Chim. Acta 471 (2002) 97–104.